Ecological Forest Management Handbook

Second Edition

Edited by Guy R. Larocque

Second edition published 2025

ISBN: 978-1-032-55517-1 (hbk)
ISBN: 978-1-032-55518-8 (pbk)
ISBN: 978-1-003-43108-4 (ebk)

16 Modeling Forest Floor Biomass and N Accumulations and Related Turnover Rates

Paul A. Arp

DOI: 10.1201/9781003431084-19

CRC Press
Taylor & Francis Group
Boca Raton London New York

CRC Press is an imprint of the
Taylor & Francis Group, an **informa** business

16 Modeling Forest Floor Biomass and N Accumulations and Related Turnover Rates

Paul A. Arp

16.1 INTRODUCTION

Knowing wood, litter, and root turnover rates is important for determining how organic matter accumulates over the years on and within mineral soils. For example, the annual forest litter and coarse woody debris accumulations determine the depth and the layering of the forest floor in terms of its litter, fermentation, and humification layers (LFH layers). Within mineral soils, roots are the dominant soil organic matter contributors by way of die-back, humification, and mineral-based organic-matter stabilization. As climate conditions vary, accumulations and turnover rates of forest organic matter (OM), including wood and roots, change as well (Bhatti et al. 2003; Deng et al. 2013). It is, however, difficult to know how extensive these changes will be and how they will accumulate over time with changing soil and site conditions across landscapes. This is because OM production and turnover times vary strongly by vegetation and by litter type composed of foliage, coarse woody debris, roots, and humus (Cou'teaux et al. 1995; Zhang et al. 2008; Jacob et al. 2010; Song et al. 2010; Ge et al. 2013).

Organic matter decomposition experiments generally aim to acquire specific information about the extent of OM loss according to prescribed experimental conditions under (i) carefully controlled temperature and moisture conditions, and/or (ii) under field conditions under changing weather and climate conditions. Such investigations vary from using bulked and unprocessed field samples to examining isolated organic matter fractions of interest. Fractioning involves physical and chemical processes, such as sample drying, grinding, and sieving, and using various solvents to isolate soluble from insoluble organic matter fractions (residues). The targets for isolation may refer to specific compound types (humin, cellulose, hemicellulose, lignin) and the extent to which these fractions are attached to mineral particles, especially clay particles. These determinations may also involve quantifying (i) the extent of organic matter mineralization, (ii) release of mineral N, Ca, Mg, K, etc. (McClaugherty 1985; Johnson and Lindberg 1992), (ii) the release of gases (NO_x, CO_2, CH_4), (iii) the change in chemical composition within the residue, and (iv) the effect of adding chemical substances or biological agents to enhance or retard the decomposition process.

Field-centered litter decomposition studies done across a wide range of field and climate conditions use single litter-filled mesh bags and spread these one by one across designated forest floor plots, and retrieve some of these each year over the course of ten years or so (Trofymow and CIDET Working Group 1998; Moore et al. 1999; Cusak et al. 2009). An alternative method uses 1 m^2 traps to collect and analyze multi-year forest litter accumulation using fiberglass screens as annual separators (Jorgensen et al. 1980; Piatek and Allen 2001). Upon retrieval, the samples are then analyzed for (i) mass remaining, (ii) nutrients remaining, and (iii) type extent of organic matter transformations.

Field-centered wood decomposition studies involve placing wood samples of same type, size, and shape into or onto the ground across many stand types. Alternatively, wood already lying on the ground can be classified by deadwood classes, and these classes are then evaluated in terms of mass loss composition over time and other parameters (e.g., Jurgensen et al. 1984; Lombardie et al. 2013).

DOI: 10.1201/9781003431084-19

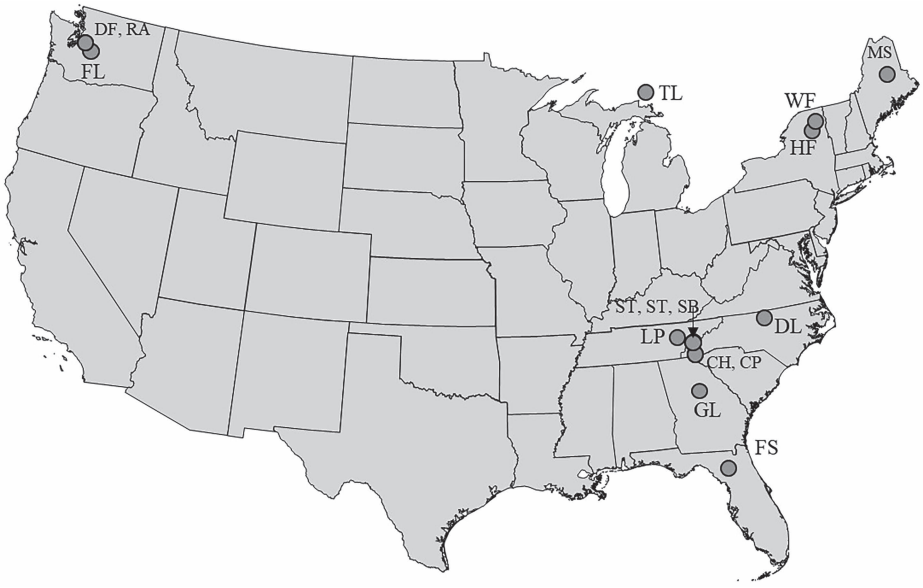

FIGURE 16.1 Locator points for the Integrated Forest Study Sites (IFS, Johnson and Lindberg 1992), overlaid on USA State Borders. There are 21 plots altogether, including two plots in Norway.

The wood decay experiment that was done across North America (LIDET 1995; Smith et al. 2011) involved wooden dowels with the lower part embedded in soil and the upper left surface exposed.

Alternative forest litter and wood studies involve (i) monitoring decomposition-generated CO_2 losses (Chiti 1999; Gaudinski et al. 2000; Song et al. 2010; Giardina et al. 2014) and (ii) radiocarbon dating (Pressenda et al. 2001). CO_2 monitoring varies from using soil-containing enclosures to whole-stand net flux determinations ranging from local to regional and global projects (Deng et al. 2013). Radiocarbon dating involves (i) determining the ^{14}C age of the decaying and humifying organic matter and (ii) tracking the decay-induced changes from the atmospheric ^{13}C as well ^{14}C concentrations (Aucour et al. 1999; Gaudinski et al. 2000; Matamala et al. 2003).

This chapter focuses on how forest floor biomass accumulation and turnover rates can be estimated across climate conditions by way of an empirical model formulation that is based on:

- Documented mass loss of CIDET and LIDET field-placed litter bags and wood blocks,
- Monitored soil respiration,
- Radiocarbon dating, and
- Mass balance modeling.

The objective of this chapter is to demonstrate how the annual accumulation of forest litter on the forest floor can be modeled to eventually reach a steady state. This demonstration is done for the Integrated Forest Site locations (IFS, Figure 16.1), as described and summarized in Johnson and Lindberg (1992). Preceding efforts to quantify some of these processes from an ecosystem modeling perspective were, e.g., summarized by Larocque et al. (2008).

16.2 MODEL FORMULATION, BACKGROUND

Modeling provides a means to integrate information generated from soil, plot, and stand-specific flux and age determinations into C-related stand- to forest-specific mass balance models (Oja and Arp 1996). This can be done by quantifying (i) the accumulating C or organic matter pools as

represented by foliage, wood, roots, forest floor, mineral soil and (ii) addressing the C allocations to each pool. For this purpose, pool sizes, net annual primary productivity, and key photosynthate allocations to foliage, wood, root, forest floor compartments all need to be estimated, and these need to be balanced with realistic estimates for turnover rates.

To quantify the decomposition process, it is generally assumed that organic matter decays in an exponential fashion, as expressed by Eq. 16.1:

$$\mathrm{SOM}(t) = \mathrm{SOM}(t_0)\ \exp\left(-\mathrm{km}(S)\ t\right) \tag{16.1}$$

where SOM(t) is the organic matter remaining at time t, $\mathrm{SOM}(t_0)$ refers to the SOM(t) production at time = 0, and km(S) is the state- and climate-dependent decomposition rate (in yr^{-1}). Apart from local climate conditions, km(S) varies by

- OM producing species,
- OM type,
- OM size and shape,
- OM composition (e.g., cellulose, hemicellulose, lignin, humin),
- OM nutrient content, especially nitrogen (N),
- OM placement (air, soil, water, from aerobic to anaerobic conditions),
- OM concentration and extent of OM compaction,
- type, diversity, and succession of OM-consuming agents (bacteria, fungi, insects, earthworms, termites).

By focusing on organic mass (M) and N alone, Zhang et al. (2007, 2008) and Smith et al. (2011) developed and analyzed the following equations:

$$\frac{dM}{dt} = -\mathrm{km}(S)M\left(1-\frac{[N]}{[N_f]}\left(1-\frac{kn}{km}\right)\right) \tag{16.2}$$

and

$$\frac{dN}{dt} = -\mathrm{kn}(S)N \tag{16.3}$$

with $k_m(S)$ and kn(S) mass and N loss coefficients further symbolized by

$$\mathrm{km}(S) = \mathrm{km}\,f(\mathrm{climate}), \tag{16.4a}$$

$$\mathrm{kn}(S) = \mathrm{kn}\,f(\mathrm{climate}), \tag{16.4b}$$

and with [N] and $[N_f]$ referring to the N concentrations within the organic matter at time t and at steady state. The climate function is given by

$$f(\mathrm{climate}) = \left[\left(\frac{\mathrm{ppt}}{1000}\right)^{0.5}\min\left(1,\frac{T_{Jul}}{T_{Jul}-T_{Jan}}\right)\right]\exp\left[-\frac{Ea}{R}\left(\frac{1}{T_{Jul}+273}-\frac{1}{288}\right)\right] \tag{16.5}$$

where ppt, T_{Jul}, and T_{Jan} refer to annual precipitation (in mm) and July and January temperatures (in ˚C). The activation energy Ea was determined to be 61,690 J $mole^{-1}$, and the universal gas constant R is given by 8.31 J $mole^{-1}$ ˚C^{-1}. In detail, Eq. 16.5 implies that organic matter composition and

N mineralization rates increase with increasing precipitation rates and with increasing July and January temperatures. In addition, f(climate) = 1 when ppt = 1,000 mm, T_{Jul} = 15°C, and T_{Jan} = 0°C.

Over the years, each year's litter contribution from leaves, wood, and root litter adds to the already existing albeit diminishing litter contributions from each of the preceding years. This realization can be summed for M and N over the years by litter type as follows:

$$M_j(\text{age}) = LP_j^0 \sum_{i=0}^{i=\text{age}} \exp\left[-km_j(S)i\right] \tag{16.6}$$

and

$$N_j = N_j^0 \sum_{i=0}^{i=\text{age}} \exp\left[-kn_j(S)i\right], \tag{16.7}$$

where i refers to litter age in years, j refers to litter type, and LP_j^0 refers to the annual litter production per litter type j. In addition, N_j^0 refers to the initial N content of LP_j^0, and $km_j(S)$ and $kn_j(S)$ are the rate of mass and N loss coefficients per litter type. The mean turnover rate for each of the accumulating litter types can then be determined from

$$MTT_j(\text{age}) = \frac{\sum_{i=0}^{i=\text{age}} i \exp\left[-km_j(S)i\right]}{\sum_{i=0}^{i=\text{soil age}} \exp\left[-km_j(S)\ i\right]}, \tag{16.8}$$

and the mean turnover rate for all organic matter accumulations for all the accumulating layers would be given by

$$MTT(\text{age}) = \frac{\sum_{j=1}^{j} \sum_{i=0}^{i=\text{age}} i \exp\left[-km_j(S)i\right]}{\sum_{j=1}^{j} \sum_{i=0}^{i=\text{soil age}} \exp\left[-km_j(S)i\right]} \tag{16.9}$$

Table 16.1 provides an overview for km and kn by forest litter type and whether placed above or within mineral soils by organic matter type and soil depth. In this, leaves, coarse woody debris, and roots all are part of the forest floor accumulations to the forest floor while root litter dominates the organic matter contributions to the mineral soil (Rasse et al. 2005). Note that litter-bag mass losses do not follow a single process over time but at least three climate- and location-specific exponential decay processes: fast, slow, and very slow (Minderman 1968). In contrast, mass losses from wooden dowels (no bark) follow a single exponential decay process. For root and wood litter, two fractions are considered, one which is generally comparable to the slow leaf litter component, and one that refers to the bark and suberized wood (bark) and root components (Matamala et al. 2003, Chen et al. 2001, Garrett et al. 2012), with the suberized portions amounting to about 10% of wood or root biomass. In general, coarse woody debris and root decay rates are quite similar, with, e.g., km (roots) = 1.4 km (coarse woody debris) according to Garrett et al. (2012). Due to increasing organic matter stabilization at increasing soil depth (Wang and Amundson 1996, Pressenda et al. 2001, Rasse et al. 2005, McFarlane et al. 2013), km needs to be adjusted by soil depth as follows:

$$km(\text{soil depth}) = km\left[1 + 0.335\,\text{soil depth}\left(\frac{\text{soil age}}{15{,}000}\right)^{\frac{1}{3}}\right] \tag{16.10}$$

TABLE 16.1
Parameters Useful for Estimating the Decay and Turnover Rates of Coarse Woody Debris, Forest Leaf Litter, and Roots in the Forest Floor and in the Mineral Soil

Forest Soil Layers	Litter Type		j	Mass Fractions	Decay Parameters	N Mineralization Parameters	Reference
Forest floor	Leaf litter	fast	1	e	$km_1 = 19.8\ km_2$	$kn_1 = kn_2\ km_1/km_2$	Zhang et al. (2007)
		slow	2	g(1-e)	$km_2 = 0.377$	$kn_2 = 0.555\ km_2\ [N]_{initial}$	
		very slow	3	(1-g) (1-e)	$km_3 = 0.292\ km_2$	$kn_3 = kn_2\ km_3/km_2$	
	Coarse woody debris	wood	4	1-f	$km_4 = 0.11$	$kn_4 = 0.35\ km_4$	Smith et al. (2011)
		bark	5	f	$km_5 = 0.292\ km_4$	$kn_5 = kn_4\ km_5/km_4$	
	Root litter	wood	6	1-f	$km_6 = 0.175$	$kn_6 = 0.35\ km_6$	Matamala et al. (2003)
		suberized	7	f	$km_7 = 0.292\ km_6$	$kn_7 = kn_6\ km_7/km_6$	
Mineral soil	Root litter	wood	8	1-f	$km_8 = 0.175$	$kn_8 = 0.35\ km_8$	Matamala et al. (2003)
		suberized	9	f	$km_9 = 0.292\ km_8/[1+0.33\ depth\ (soil\ age/15{,}000)^{0.33}]$	$kn_9 = kn_8\ km_9/km_8$	Wang et al. (1996), interpreted from graph

For leaf litter fractions and related e and g specifications, see Zhang et al. (2007); f refers to the suberized component of coarse woody debris (bark) and root litter. Also note: [N]initial = [N0], in %.

where the soil age component reflects cumulative retention and organo-metal stabilization of soil leached C. In addition, root litter production and accumulations decrease with increasing soil depth, as follows (Jackson et al. 1996):

$$\text{Cumulative fraction of } LP_{roots} = 1 - b^{\text{ soil depth}}, \tag{16.11}$$

with b varying from 0.914 (tundra) to, e.g., 0.943 (boreal forest) and 0.976 (temperate coniferous forest).

16.3 COMPUTATIONS

The computations, done for each IFS location and plot, were initially based on Eqs 16.1 to 16.9. The computational process was facilitated using the STELLA modeling software. The resulting calculations were done by year from time = 0 up to 2,000 years so that the steady-state condition for the forest floor biomass and N accumulations could be emulated for each location through calibration. The Runge-Kutta algorithm was used to ensure numerical stability. During the calibration process, it was realized that Eqs 16.2 and 16.3 needed to be reformulated to best capture the gradual conversion of fresh forest litter toward the steady-state forest floor forest biomass and N accumulations at each IFS location as follows:

$$\frac{dM}{dt} = -km(S)M\left(1-\alpha\frac{[N]}{[N_f]}\left(1-\frac{\beta kn}{km}\right)\right) \tag{16.12}$$

and

$$\frac{dN}{dt} = -\beta kn(S)N, \tag{16.13}$$

where α and β serve as plot-specific biomass and N mineralization adjustment parameters. For example:

(i) Reducing β toward 0 lowers the expected N mineralization rate but increases the expected biomass mineralization rate;

(ii) Setting β kn/km = 1 or α = 0 renders the biomass mineralization process independent of the N mineralization process;

(iii) At steady-state, the $1-\alpha\frac{[N]}{[N_f]}\left(1-\frac{\beta kn}{km}\right)$ expression simplifies to $1-\alpha\left(1-\frac{\beta kn}{km}\right)$.

The process of the changing N concentrations in the forest floor would occur as follows:

$$dN/dM = \frac{\beta kn}{km}[N]/\left[1-\pm\frac{[N]}{[N_f]}\left(1-\frac{\beta kn}{km}\right)\right]. \tag{16.14}$$

Consequently,

(i) when km = β kn, then $dN/dM = \frac{\beta kn}{km}[N]$;

(ii) when dN / dM < 1, M losses exceed N losses, so that [N] increases, and C/N decreases;

(iii) when dN / dM > 1, N losses exceed M losses, so that [N] decreases, and C/N increases.

At steady state, the M and N additions to the forest floor equal the M and N losses from the forest floor. For this condition—and noting from Table 16.1 that $kn/km = kn_1/km_1 = kn_2/km_2 = kn_3/km_3 = 0.555\,[N_0]$—it can be shown via Eqs 16.12 and 16.13 that

$$[N_f] = \frac{1-\alpha(1-0.555[N_0])}{0.555\beta} \tag{16.15}$$

and that

$$\alpha = \frac{1-0.555\,\beta[N_f]}{1-0.555\,\beta[N_0]} \tag{16.16}$$

Hence, α can be inferred from steady-state forest litter $[N_0]$ and forest floor $[N_f]$ concentrations, and from plot-based model-calibrated β values. In addition, β can be estimated from the steady-state N_0, N_f (t/ha) and $[N_0]$ (%) specifications by setting

$$\beta \approx 10\frac{N_0}{N_f\ f(clim)[N_0]}. \tag{16.17}$$

16.4 RESULTS AND DISCUSSION

The summary in Table 16.2 demonstrates that the IFS locations represent a wide range of forest type by tree age, climate condition, forest litter production, forest floor biomass and N accumulations, and related N concentrations and C/N ratios. Note that the C/N ratios generally decrease as the forest litter accumulations age, but exceptions of this occurred at the American beech (SB1, SB2) and red alder (RA) locations. At the CP pine location, the C/N ratio remained the same

TABLE 16.2

Leaf Area Index (LAI), Tree Age, Climate Conditions, and Forest Litter and Forest Floor Biomass Accumulation Including N Concentrations and C/N Ratios at the IFS Locations, with Information on Two Additional DL Plots (DL19, DL40, Jorgensen et al. 1980)

									Forest Litter				Forest Floor			
			LAI	Age	Tjan	Tjul	Precip.	f(climate)	Biomass	Litter N			Biomass	Forest Floor N		
Loc	Forest Type	Site	m^2/m^2	Years	˚C	˚C	mm	-	t/ha	t/ha	%	C/N	t/ha	t/ha	%	C/N
CP	White Pine	Plantation	17	30	1.3	20.9	1440	2.00	6.47	0.0431	0.666	75.1	28.1	0.282	1.003	49.9
DF	Douglas Fir	Plantation	5.3	55	3	16.5	1140	1.22	1.78	0.0148	0.831	60.1	36.7	0.379	1.033	48.4
DL	Loblolly pine	Plantation	6.5	23	3	25.2	1130	2.54	4.92	0.0187	0.380	131.4	63.0	0.450	0.714	70.0
FS	Slash Pine	Plantation	5.1	22	12.2	27.1	1120	2.96	4.45	0.0215	0.483	103.6	37.4	0.286	0.765	65.4
GL	Loblolly pine	Plantation	11	17	6.7	26.8	870	2.54	10.32	0.0760	0.737	67.9	32.7	0.310	0.948	52.8
LP1	Loblolly pine	Plantation	3.6	35	2	24.7	1140	2.45	2.60	0.0137	0.528	94.7	14.1	0.277	1.960	25.5
LP2	Loblolly pine	Plantation	3.6	35	2	24.7	1140	2.45	3.50	0.0194	0.554	90.2	14.1	0.277	1.960	25.5
NS1	Norway Spruce	Plantation	10.5	40	-6.9	16	1070	0.79	3.29	0.0287	0.873	57.2	63.3	0.842	1.330	37.6
NS2	Norway Spruce	Plantation	10.5	40	-6.9	16	1070	0.79	2.29	0.0203	0.886	56.4	57.8	0.605	1.048	47.7
CH	Tol. Hardwoods	Second growth	–	10	1.3	20.9	1380	1.96	4.98	0.0364	0.731	68.4	27.3	0.245	0.897	55.7
TL	Tol. Hardwoods	Second growth	5.3	135	-12.4	16	1210	0.68	3.73	0.0400	1.072	46.6	33.0	0.927	2.809	17.8
HF	Tol. Hardwoods	Old growth	6.5	100	-9.4	17.5	970	0.80	5.26	0.0596	1.132	44.2	44.9	0.531	1.182	42.3
SB1	Tol. Hardwoods	Old growth	–	200	-1.6	18.7	1510	1.56	2.24	0.0262	1.168	42.8	29.1	0.232	0.798	62.6
SB2	Tol. Hardwoods	Old growth	–	200	-1.6	18.7	1510	1.56	1.83	0.0234	1.280	39.1	28.8	0.247	0.857	58.3
RA	Red Alder	Old growth	4.5	55	3	16.5	1140	1.22	4.48	0.0800	1.785	28.0	98.5	1.629	1.654	30.2
FL	Silver Fir	Old growth	–	180	-3.9	12.7	1740	0.82	2.73	0.0165	0.604	82.7	54.8	0.575	1.049	47.7
WF	Mixed	Old growth	8.2	100	-12.6	14.3	1150	0.54	2.60	0.0237	0.913	54.8	141.4	2.642	1.868	26.8
MS	Red spruce	Old growth	5.7	85	-10.3	19.4	990	0.95	2.11	0.0122	0.580	86.3	150.7	1.121	0.744	67.2
SS	Red Spruce	Old growth	–	250	-3	17.1	1510	1.26	1.91	0.0112	0.587	85.2	166.1	1.916	1.154	43.3
ST1	Red Spruce	Old growth	9	250	-1.7	17.1	2440	1.71	1.77	0.0130	0.734	68.1	151.1	2.162	1.431	34.9
ST2	Red Spruce	Old growth	9	250	-1.7	17.1	2440	1.71	5.42	0.0323	0.596	83.8	108.9	1.517	1.393	35.9
DL19	Loblolly pine	Plantation	–	19	3	25.2	1130	2.54	7.71	0.0626	0.812	61.6	29.0	0.397	1.367	36.6
DL40	Loblolly pine	Plantation	–	40	3	25.2	1130	2.54	6.09	0.0409	0.671	74.5	32.9	0.416	1.266	39.5

while the lowest forest floor C/N ratio was recorded for the tolerant hardwood site at the Turkey Lakes (TL) location.

The numbers in Table 16.3 refer to:

(i) the best-fitted α and β values that account for the location-by-location variations pertaining to the model-emulated rates of litter decay and N mineralization,
(ii) the best-fitted forest floor biomass and N turnover times at (a) the mean turnover times and (b) reported tree age, and
(iii) the model-inferred forest flood decomposition index, given by:

$$\text{FFDI} = 1-\alpha\,(1-0.555\,\beta\,[N_0]),\ \text{with}\,[N_0]\ \text{in}\ \%$$

An example of how the model-calculated forest floor biomass, N content, N concentration, and related C/N ratio all vary over time starting from time = 0 and by changed mean annual temperature (ΔT = –5, 0, 5 ˚C) and precipitation (ΔPPT = 0, 500 mm) is presented in Figure 16.2 for the TL location. As shown, the forest-floor biomass accumulations and related C/N ratios are modeled to decrease with increasing mean annual temperatures and precipitation rates while the N concentrations would increase. In biological terms, the rate of decay of the accumulating forest floor biomass is modeled to decrease as the availability of digestible C sources diminishes. This therefore leads to increasing N concentrations and decreasing C/N ratios. Decreasing C/N ratios, however, also lead to decreasing N retention. As a result, reported N leaching rates increase at locations with low forest floor C/N ratios, as detailed for the TL location by, e.g., Foster et al. (1992), Moayeri et al. (2001), and Murphy et al. (2009). In comparison, the reported N leaching rates were found to be low at the hardwood-covered Huntington Forest (HF) and the Great Smoky Mountains beech locations (SB1/SB2: Johnson and Lindberg 1992). The contrast between the TL and HF hardwood locations is striking: both accumulate forest biomass toward the steady-state conditions with about the same turnover times (15.5 versus 12.3 years, respectively, Table 16.3) but not so for N content (33.1 vs. 12.7 years, respectively; Table 16.3). Hence, forest floor N% increases slightly at HF but nearly triples at TL (Table 16.3, Figure 16.3). One reason for this difference could be related to the higher calcareousness of the TL soil parent material, which therefore implies higher biological activities and biomass turnover rates at TL compared to HF. In some cases, the forest litter to forest floor C/N ratio is about 1 (CP, white pine; RA, red alder) or increases to 1.6 (SB1, SB2, beech). This implies that biological activities at these locations consume forest litter N at the same or a higher rate than forest litter C.

The forest floor-to-forest litter C/N ratio appears to decrease with increasing forest litter C/N ratio from the IFS hardwood through the spruce-fir to the pine plantation locations as shown in Figure 16.4. In this, the forest floor-to-forest litter C/N ratio variations are largest for the hardwood locations (ranging from 0.4 to 1.5) and are least for the spruce-fir locations (ranging from 0.4 to 0.8). In contrast, the forest litter C/N ratio variations are largest for the pine plantation locations, spanning from 0.6 to 1.37. For the spruce-fir locations, the forest floor-to-forest litter C/N ratio appears to decrease with increasing tree age, but this is not the case for the hardwood and pine plantation locations (Table 16.2).

Figure 16.5 shows how the best-fitted N mineralization adjustment parameter α varies with the best-fitted biomass mineralization parameter β (left) and the Table 16.2 specified C/N ratio of the forest litter (right). The resulting patterns reveal again noticeable α-versus-β differences for the IFS hardwood, spruce-fir, and pine plantation locations. In addition, there is a significant decrease in the best-fitted N mineralization parameter (α) as the forest litter C/N ratio increases from the hardwood through the spruce-fir to the pine plantation locations, in which the TL and DL locations are recognizable outlier. The patterns displayed also reveal that the plot-to-plot α and β variations for the LP,

TABLE 16.3

Best-Fitted Calibration Parameters (α, β), Turnover Times, and Model-Assessed Forest Floor Biomass and N Accumulations at Turnover Time and IFS-Quoted Tree Age, Tree Age When 90% and 95% of Estimated Steady-State Forest Biomass Is to Occur, and Model-Generated Forest Floor Decomposition Index FFDI, for Each IFS Location

			Forest Floor Decomposition Adjustment Parameters	Forest Floor Turnover Times For: N		Estimated Forest Floor Biomass and N at Turnover Time:				Best-Fitted Forest Floor Biomass at Tree Age	Tree Age When Reported Biomass Is Modeled to Occur at:	Forest Floor Decomposition Index (FFDI) = 1-α (1-β kn/km)	Biomass	N	Biomass
	Forest	Site				α	β	Years	Years						
Location	Type	Condition	% Reported	t/ha	%	90%	95%	CP	White Pine	Plantation	0.610	1.15	7.8	9.2	19
67.6	0.18	63.8	27.2	96.7	18	25	0.523	DF	Douglas Fir	Plantation	0.938	0.44	34	35.7	24.2
65.9	0.251	66.2	29.5	80.4	62	110	0.252	DL	Loblolly Pine	Plantation	0.912	0.43	30.7	33.3	41.7
66.2	0.328	72.9	36.2	57.5	77	104	0.171	FS	Slash Pine	Plantation	0.903	0.53	17.3	18.7	24.5
65.5	0.189	66.1	27.5	73.5	42	58	0.225	GL	Loblolly pine	Plantation	0.675	1.30	5.3	6.2	21.5
65.7	0.202	65.2	31.2	95.4	13	21	0.684	LP1	Loblolly pine	Plantation	0.660	0.38	20.1	28.1	9.8
69.3	0.182	65.7	11.6	82.1	44	75	0.413	LP2	Loblolly pine	Plantation	0.517	0.52	12.3	19.9	10.1
71.5	0.181	65.3	12.9	91.1	32	48	0.566	NS1	Norway Spruce	Plantation	0.835	0.495	35.6	40.5	42.5
67.2	0.552	65.6	44.4	70.2	113	120	0.366	NS2	Norway Spruce	Plantation	0.944	0.48	39.5	41.2	38
65.8	0.393	65.0	38.3	66.3	85	128	0.279	CH	Tol. Hardwoods	Second growth	0.844	1	9.2	10.2	18.3
67.0	0.165	67.3	19.1	70.0	20	24	0.498	TL	Tol. Hardwoods	Second growth	0.352	0.48	18.6	33.7	23.2
70.3	0.607	65.5	32.8	99.4	45	37	0.748	HF	Tol. Hardwoods	Old growth	0.839	1.25	12.3	12.7	29.5
65.7	0.352	66.3	44.9	99.9	29	39	0.820	SB1	Tol. Hardwoods	Old growth	1.224	0.64	13.1	12.4	18.1
62.3	0.15	64.7	29.1	100.1	33	42	0.283	SB2	Tol. Hardwoods	Old growth	1.166	0.47	15.6	15.3	18
62.5	0.165	66.8	28.8	100.0	36	51	0.224	RA	Red Alder	Old growth	1.022	0.23	28.2	28	61
61.9	1.059	65.0	83.4	84.7	69	91	0.211	FL	Silver Fir	Old growth	0.820	0.585	41.3	47.9	36.5
66.6	0.374	65.0	53.3	97.3	105	144	0.341	WF	Mixed	Old growth	0.895	0.18	135.5	149.9	93
65.8	1.712	64.8	80.5	56.9	345	466	0.187	MS	Red Spruce	Old growth	0.981	0.198	124.1	126.3	98.6
65.4	0.733	65.4	81.3	54.0	304	408	0.082	SS	Red Spruce	Old growth	0.974	0.0795	228.4	234	108
64.8	1.254	65.4	113.2	68.2	564	750	0.051	ST1	Red Spruce	Old growth	0.981	0.0482	222.2	227.1	99.3
65.7	1.411	65.3	104.9	69.4	535	708	0.038	ST2	Red Spruce	Old growth	0.900	0.21	59	64.8	72
66.1	0.994	65.5	106.0	97.3	149	202	0.162	DL19	Loblolly pine	Plantation	0.644	0.76	7.2	9.3	19.4
66.8	0.184	46.3	26.6	91.6	17	24	0.577	DL40	Loblolly pine	Plantation	0.653	0.755	11.8	14.4	22.2
67.6	0.242	58.2	31.1	94.6	30	41	0.530								

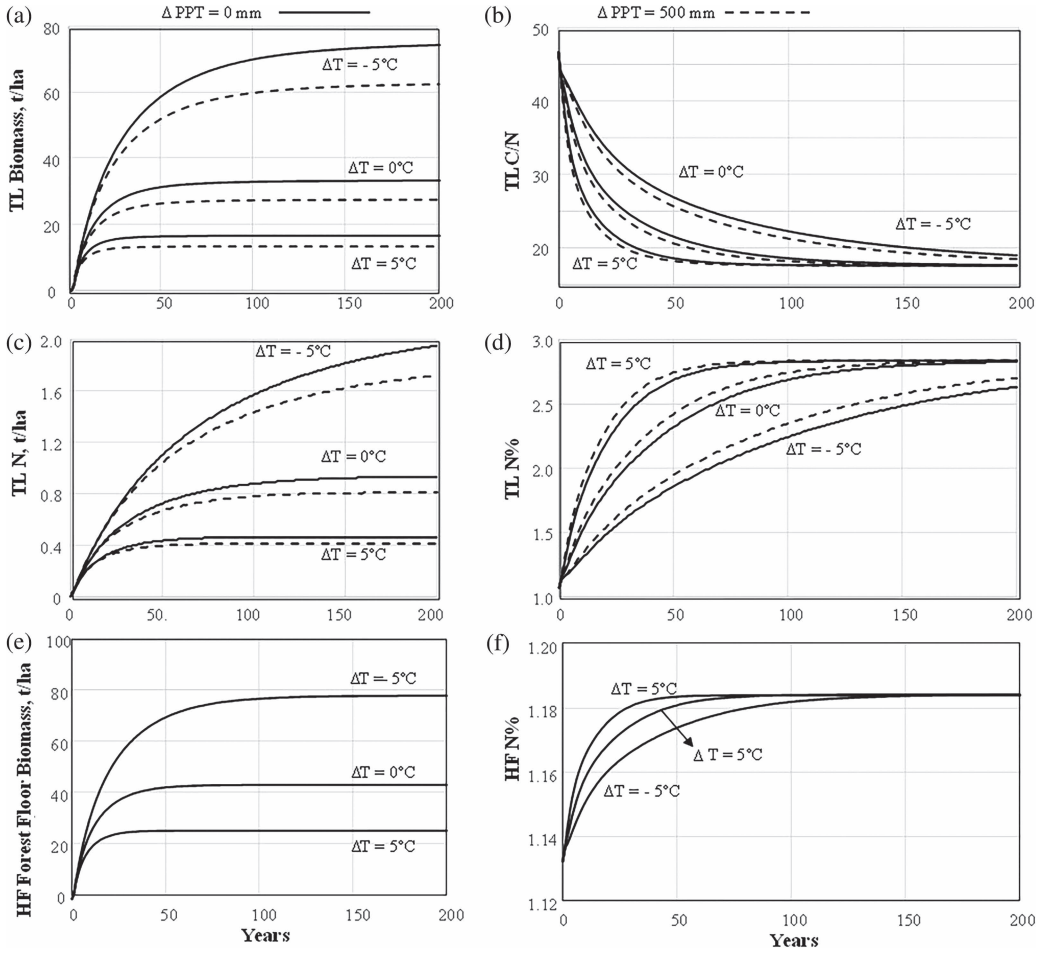

FIGURE 16.2 Modeled forest floor biomass (**A**) and nitrogen accumulations (**B**) along the y-axis in tonnes/ha for the Turkey Lakes (TL) location over 200 years (x-axis), assuming constant forest litter input from year to year as specified in Table 16.1. Also shown for the same location: related changes in C/N ratio (**C**) and N% (**D**) for the forest floor. For comparison, the corresponding forest floor biomass and N% concentrations are shown for the Huntington Forest location (HF) at bottom left (**E**) and right (**F**).

NS, and SB Plot 1 and Plot 2 locations are considerably smaller than the wider location-to-location variations. This is also true for the DL19 and DL40 locations of the Jorgensen et al. (1980) report but not so for the IFS-reported DL location (tree age = 23 years). For the latter, the forest floor C/N ratio is exceptionally high while the parameters for biomass and N mineralization are exceptionally low.

Figure 16.6 shows that the results so achieved are in general agreement with the sequential 8-year forest floor biomass and mineralization results reported by Jorgensen et al. (1980) for the DL19 and DL40 loblolly pine locations within the Duke Forest of Northern Carolina. Similar agreements were achieved for the loblolly pine forest floor biomass and mineralization results reported by Piatek and Allen (2001).

The scatterplot in Figure 16.7 shows that IFS-reported forest floor biomass at IFS-reported tree age generally exceeds modeled forest floor biomass by 36% and does not fall below the 1:1 line. Greater than modeled forest biomass accumulations are likely due to antecedent forest floor biomass prior to forest cover reestablishment. In contrast, the model calculations start at zero forest floor biomass at zero forest age.

The turnover times of the accumulating forest floor biomass and N are plotted in Figure 16.8 for each IFS location, grouped by forest type. These times are similar for the pine plantations and the tolerant hardwood sites while the reported tree age range is much wider for the latter. In contrast, the modeled turnover times are widest for the spruce-fir locations, likely due to the higher spruce-firlignin content.

Figure 16.9 shows how the forest biomass and N accumulate over time at the three DL locations overall and at modeled turnover times. In general, the biomass and N accumulations so derived amount to 66.2 ± 2.3% and 64.7 ± 4.6% of the biomass and N accumulations at steady state (see Table 16.3).

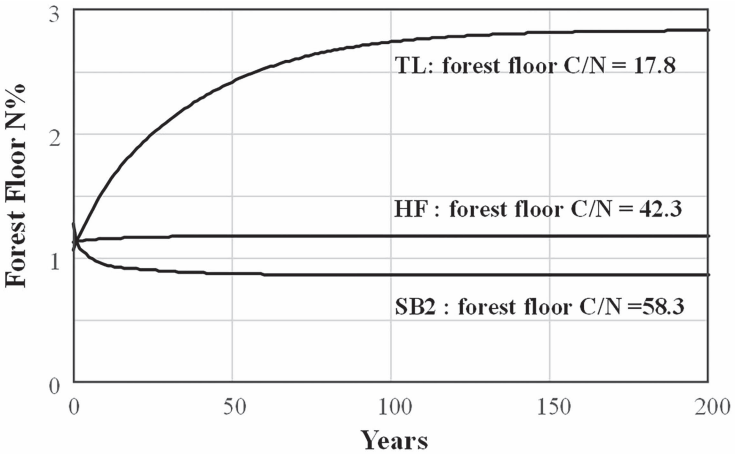

FIGURE 16.3 Modeled forest floor N% changes (y-axis) over time (x-axis) at the Turkey Lakes (TL), Huntington Forest (HF), and Great Smoky Mountains Beech (SB) locations, as implied by the low C/N = 17.8 ratio at TL (where N% increases), the CN = 42.3 ratio at HF (where N% stays the same), and the CN = 58.3 at SB (where N% decreases).

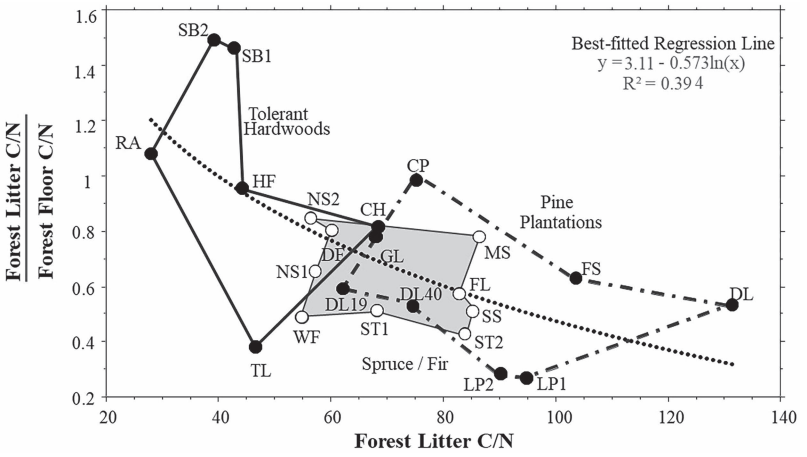

FIGURE 16.4 Dot plot showing the ratio of the forest litter C/N ratio over the forest floor C/N ratio (y-axis) against the forest floor C/N ratio (x-axis) at each IFS location. These dots are joined by polygons to reveal the dot-implied pattern by forest type, i.e., tolerant hardwoods (thick solid line, mostly at left), spruce-fir combinations (thin solid line, at center), and pine plantation (thick stippled line, mostly at right). Also overlaid is the best-fitted y-versus-x regression line (dotted points).

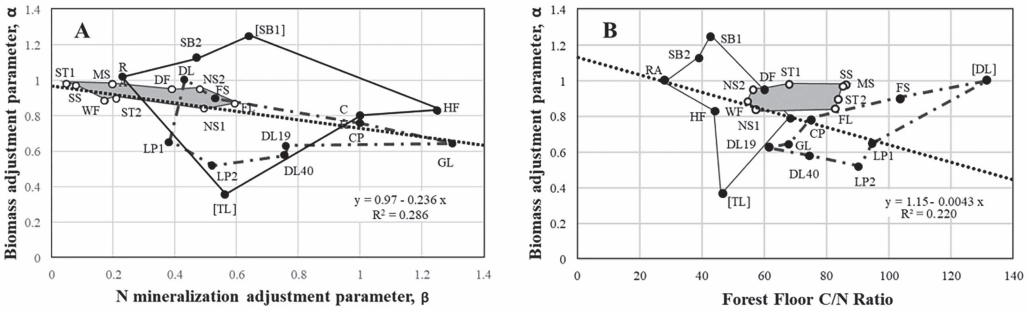

FIGURE 16.5 Dot plotting the biomass-adjustment parameter α versus (i) the N-adjustment parameter β (**Panel A**) and (ii) versus the forest litter C/N ratio (**Panel B**) for the IFS locations, polygon-joint by hardwood, spruce-fir, and pine plantation locations, as in Figure 16.4. Also shown are the best-fitted y-versus-x regression lines.

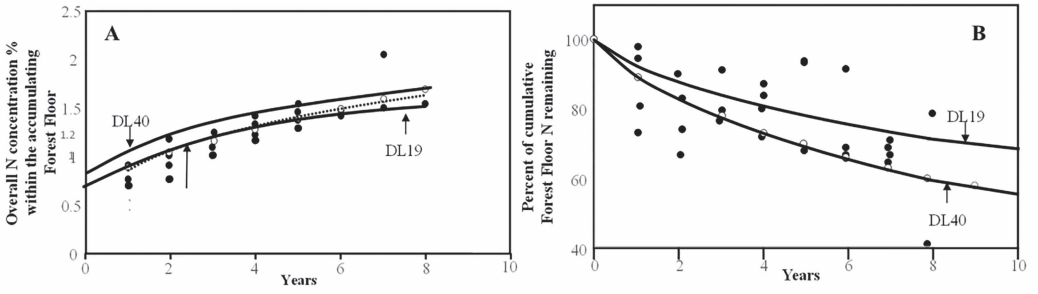

FIGURE 16.6 Actual (black dots) and modeled (heavy black lines) forest floor N concentrations (**Panel A**) and percent of N remaining (**Panel B**) within the sequentially accumulated forest litter at the Duke Forest DL19 and DL40 loblolly pine plantations (y-axes), plotted over the course of eight years (x-axis). Black dots: taken from Jorgensen et al. (1980); open dots with point-stippled lines: best-fitted y-versus-x regression model through the black dots.

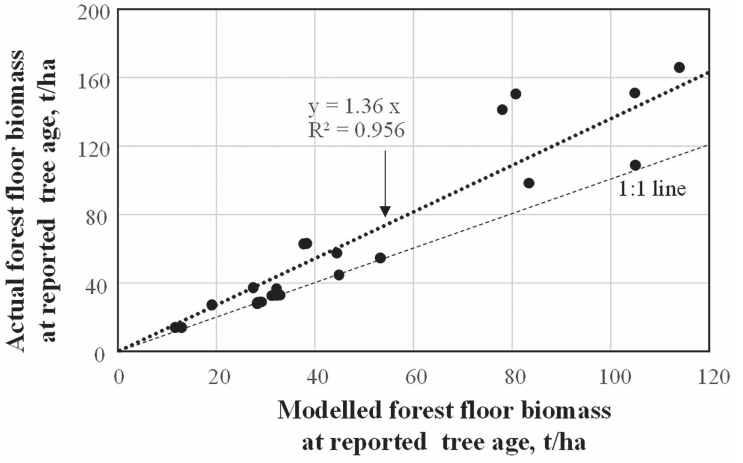

FIGURE 16.7 Dot plot of actual (y-axis) versus best-fitted (x-axis) forest floor biomass at reported tree age for each IFS location, with best-fitted regression equation and 1:1 line overlaid. On average, the reported biomass at tree age exceeds the modeled biomass by 36%.

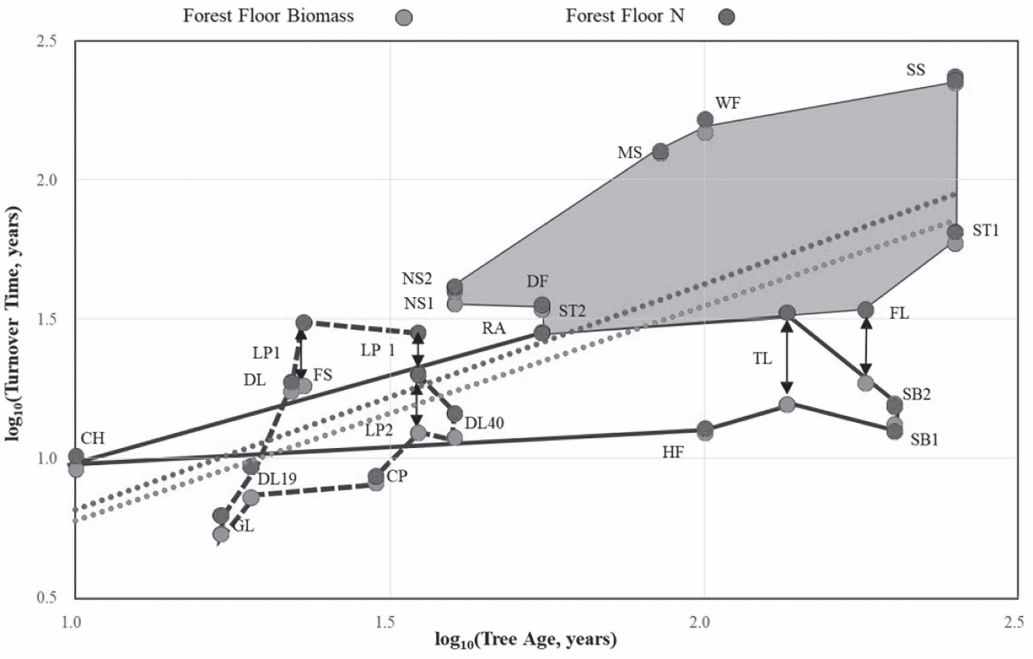

FIGURE 16.8 Log-log plot of forest-floor biomass (grey dots) and N turnover (black dots) times (y-axis) versus reported tree age (x-axis), with dots polygonized by forest type, i.e., tolerant hardwoods (thick solid line), spruce-fir combinations (thin solid line), and pine plantations (thick stippled line).

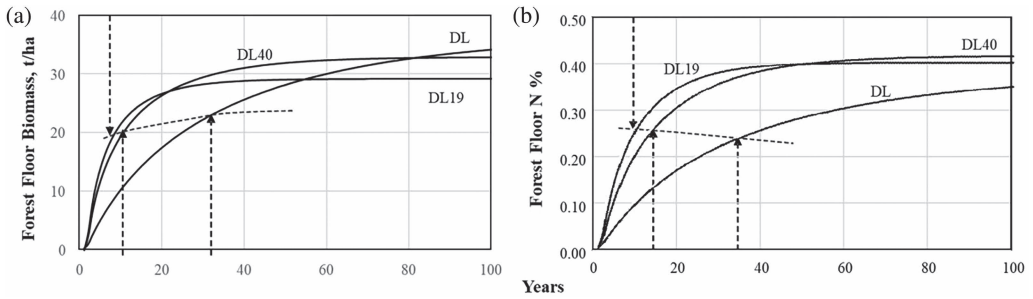

FIGURE 16.9 Line plots for modeled forest floor biomass (**Panel A**) and N% (**Panel B**) along the y-axes versus year along the x-axes at the Duke forest DL, DL19 and DL40 pine plantation plots, assuming constant litter production rates, initially falling on bare ground and at model-generated arrow-indicated turnover times.

Based on the report by Berg (2000) and the earlier results, there appears to be a general association between the forest floor decomposition index FFDI, litter lignin % and litter N % by forest type (Figure 16.10). While not in exact correspondence, the FFDI and lignin % versus forest plots have

(i) the widest variations across hardwood litter,
(ii) the least variations across spruce-fir litter, and
(iii) generally the lowest litter N% levels across the pine plantations.
(iv) a high 20–50% lignin range which, in part, refers to the final lignin content of decomposed forest litter, i.e., [N_f].

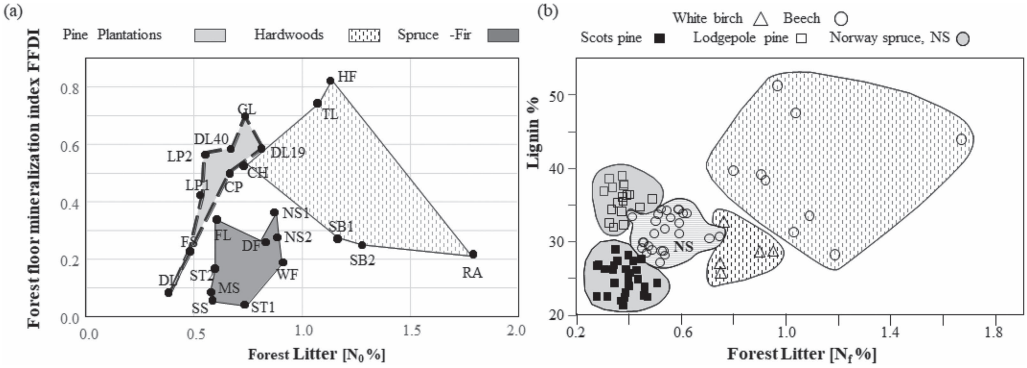

FIGURE 16.10 Polygonized dot plots of (i) the model-generated forest floor decomposition index FFDI = 1–α (1–0.555 $\beta[N_0]$) for the IFS locations (**Panel A**), and (ii) reported lignin% (Berg 2000; **Panel B**) versus the initial and final N concentrations of the decomposing forest litter along the x-axes, by forest type. $[N_0]$ = initial forest litter N concentration; [Nf]= final forest litter N concentration.

Figure 16.10 therefore implies that the 0.2–1.8 N% range is in part due to increasing N retention with increasing lignin %, but with hardwood litter exhibiting wider initial and final N% ranges than spruce and pine litter (Berg 2000; Kreutzweiser et al. 2008; Wang et al. 2021).

16.5 CONCLUDING REMARKS

At the base of tracking changes in forest floor biomass and nitrogen accumulations over time is the CIDET-generated parametrization of fast, slow, and very slow forest litter decaying processes, as affected by litter type and climate (Table 16.1). While it is assumed that annual per hectare forest litter productions remain the same year after year, they differ substantially across the IFS locations (Table 16.2). The assumption of constant litter production per year is, however, not mandatory, because the model formulation can accommodate changing forest litter production rates if tracked or projected over time based on actual or projected climate and forest disturbance patterns.

To further generalize, the model can be applied to many more forest locations for which summaries regarding forest litter production, forest floor biomass (e.g., Reichle 1981) and N accumulations are also available. In addition, the formulation can be used to track other nutrients such as Ca, Mg, K, P, and S, and there is the need to address wood and root decay above and within the mineral soil as well. In this regard, Tables 16.1, 16.2, and 16.3 provide a starting point for quantifying long-term forest type and location-specific production and related above- and below-ground decay differences at the per hectare level.

As illustrated, the proposed model provides an efficient means to ascertain forest floor biomass and N turnover times: only one parameter (β) needs to be calibrated once reported or expected forest litter production and forest floor biomass and N accumulations are specified. The resulting model-estimated turnover rates are generally but not always somewhat slower for N than for biomass. Over time, the model consistently projects 62% to 64% of the tree-age reported biomass and N accumulations. This difference is in part due to setting modelled biomass and N content to 0 at time 0.

REFERENCES

Aucour, A.M., R. Bonnefille, and C. Hillaire-Marcel. 1999. Sources and accumulation rates of organic carbon in an equatorial peat bog (Burundi, East Africa) during the Holocene: carbon isotope constraints. *Palaeogeogr. Palaeoclimatol. Palaeoecol.* 150:179–189.

Berg, B. 2000. Litter decomposition and organic matter turnover in northern forest soils. *For. Ecol. Manag.* 133:13–22.

Bhatti, J.S., G.C. van Kooten, M.J. Apps, et al. 2003. Carbon balance and climate change in boreal forests. Chapter 20. In *Towards sustainable management of the boreal forest,* eds. P.J. Burton, C. Messier, D.W. Smith, et al., pp. 799–855. Ottawa, Ontario, Canada: NRC Research Press.

Chen, H., M.E. Harmon, and R.P. Griffiths. 2001. Decomposition and nitrogen release from decomposing woody roots in coniferous forests of the Pacific Northwest: A chronosequence approach. *Can. J. For. Res.* 31:246–260.

Chiti, T., R.E.M. Neubert, I.A. Janssens, et al. 1999. Radiocarbon dating reveals different past managements of adjacent forest soils in the Campine region, Belgium. *Chem. Geol.* 159:87–105.

Cou'teaux, M.-M., P. Bottner, and B. Berg. 1995. Litter decomposition, climate and litter quality. *Trends Ecol. Evol.* 10:63–66.

Cusack, D.A.F., W.W. Chou, W.H. Yang, et al. 2009. Controls on long-term root and leaf litter decomposition in neotropical forests. *Glob. Change Biol.* 15:1339–1355.

Deng, F., J.M. Chen, Y. Pan, et al. 2013. The use of forest stand age information in an atmospheric CO2 inversion applied to North America. *Biogeosciences* 10:5335–5348.

Foster, N., M. Mitchell, I. Morrison, et al. 1992. Cycling of acid and base cations in deciduous stands of Huntington Forest, New York, and Turkey Lakes, Ontario. *Can. J. For. Res.* 22:167–174.

Garrett, L.G., M.O. Kimberley, G.R. Oliver, et al. 2012. Decomposition of coarse woody roots and branches in managed Pinus radiata plantations in New Zealand—A time series approach. *For. Ecol. Manag*. 269:116–123.

Gaudinski, J.B., S.E. Trumbore, E.A. Davidson, et al. 2000. Soil carbon cycling in a temperate forest: radiocarbon-based estimates of residence times, sequestration rates and partitioning of fluxes. *Biogeochemistry* 51:33–69.

Ge, X., L. Zeng, W. Xiao, et al. 2013, Effect of litter substrate quality and soil nutrients on forest litter decomposition: A review. *Acta Ecol. Sin*. 33:102–108.

Giardina, C.P., C.M. Litton, S.E. Crow, et al. 2014. Warming-related increases in soil CO2 efflux are explained by increased below-ground carbon flux. *Nat. Clim. Chang.* 4:822–827.

Jackson, R.B., J. Canadell, J.R. Ehleringer, et al. 1996. A global analysis of root distributions for terrestrial biomes. *Oecologia* 108:389–411.

Jacob, M., K. Viedenz, A. Polle, et al. 2010. Leaf litter decomposition in temperate deciduous forest stands with a decreasing fraction of beech (*Fagus sylvatica*). *Oecologia* 164:1083–1094.

Johnson, D.W., and S.E. Lindberg, eds. 1992. *Atmospheric deposition and forest nutrient cycling: A synthesis of the integrated forest study*. Ecological Studies 91. New York, NY: Springer-Verlag.

Jorgensen, J.R., C.G. Wells, and L.J. Metz. 1980. Nutrient changes in decomposing loblolly pine forest floor. *Soil Sci. Soc. Am. J.* 44:1307–1314.

Jurgensen, M.F., M.J. Larsen, S.D. Spano, et al. 1984. Nitrogen fixation associated with increased wood decay in Douglas-fir residue. *For. Sci*. 30:1038–1044.

Kreutzweiser, D.P., K.P. Good, S.S. Capell, et al. 2008. Leaf-litter decomposition and macroinvertebrate communities in boreal forest streams linked to upland logging disturbance. *J. North Am. Benthol. Soc.* 27:1–15.

Larocque, G.R., J.S. Bhatti, A.M. Gordon, et al. 2008. Uncertainty and sensitivity issues in process-based models of carbon and nitrogen cycles in terrestrial ecosystems. In *Environmental modelling, software and decision support,* ed. A.J. Jakeman, pp. 307–368. Amsterdam: Elsevier.

LIDET. 1995. *Meeting the challenges of long-term, broad-scale ecological experiments.* Report No. 19. US LTER Network Office, Seattle.

Lombardi F., P. Cherubini, R. Tognetti, et al. 2013. Investigating biochemical processes to assess deadwood decay of beech and silver fir in Mediterranean mountain forests. *Ann. For. Sci.* 70:101–111.

Matamala, R., M.A. Gonzalez-Meler, J.D. Jastrow, et al. 2003. Impacts of fine root turnover on forest NPP and soil C sequestration potential. *Science* 302 (ANL/ER/JA-47577).

McClaugherty, C.A., J. Pastor, J.D. Aber, et al. 1985. Forest litter decomposition in relation to soil nitrogen dynamics and litter quality. *Ecology* 66:266–275.

McFarlane, K.J., M.S. Torn, P.J. Hanson, et al. 2013. Comparison of soil organic matter dynamics at five temperate deciduous forests with physical fractionation and radiocarbon measurements. *Biogeochemistry* 1:457–476.

Minderman, G. 1968. Addition, decomposition and accumulation of organic matter in forests. *J. Ecol.* 56:355–362.

Moayeri, M., F.-R. Meng, P.A. Arp, et al. 2001. Evaluating critical soil acidification loads and exceedances for a deciduous forest at the turkey lakes watershed. *Ecosystems* 4:555–567.

Moore, T.R., J.A. Trofymow, B. Taylor, et al. 1999. Litter decomposition rates in Canadian forests. *Glob. Change Biol.* 5:75–82.

Murphy, P.N.C., M. Castonguay, J. Ogilvie, et al. 2009. A geospatial and temporal framework for modeling gaseous N and other N losses from forest soils and basins, with application to the Turkey Lakes Watershed Project, in Ontario, Canada. *For. Ecol. Manag.* 258:2304–2317.

Oja, T., and P.A. Arp. 1996. Nutrient cycling and biomass growth at a North American hardwood site in relation to climate change: FORSVA assessments. *Clim. Change* 34:239–251.

Piatek, K.B., and H.E. Allen. 2001. Are forest floors in mid-rotation stands of loblolly pine (*Pinus taeda*) a sink for nitrogen and phosphorus? *Can. J. For. Res.* 31:1164–1174.

Pressenda, L.C.R., S.E.M. Gouveia, and R. Aravena. 2001. Radiocarbon dating of total soil organic matter and humin fraction and its comparison with ^{14}C ages of fossil charcoal. Proceedings of the 17th International 14 C Conference; I Carmi and E Boaretto eds. *Radiocarbon* 43:595–601.

Rasse, D.P., C. Rumpel, and M.F. Dignac. 2005. Is soil carbon mostly root carbon? Mechanisms for a specific stabilisation. *Plant Soil* 269:341–356.

Reichle, D.E. 1981. Dynamic properties of forest ecosystems. *Int. Biol. Programme 23*.

Smith, A.C., J.S. Bhatti, H. Chen, et al. 2011. Modelling above-and below-ground mass loss and N dynamics in wooden dowels (LIDET) placed across North and Central America biomes at the decadal time scale. *Ecol. Model.* 14:2276–2290.

Song, F., Z. Fan, and R. Song. 2010. Review of mixed forest litter decomposition researches. *Acta Ecol. Sin.* 30:221–225.

Trofymow, J.A. 1998. *The Canadian Intersite Decomposition Experiment (CIDET): Project and site establishment report*. CIDET Working Group. Natural Resources Canada, Canadian Forest Service, Pacific Forest Center, Victoria, B.C.; Inf. Rep. BC-X-378.eorest

Wang, Y., and R. Amundson. 1996. Radiocarbon dating of soil organic matter. *Quat. Res.* 45:282–288.

Wang, Q.W., M. Pieristè, C. Liu, et al. 2021. The contribution of photodegradation to litter decomposition in a temperate forest gap and understorey. *New Phytol.* 229:2625–2636.

Zhang, C.F., F.R. Meng, J.S. Bhatti, et al. 2008. Modeling forest leaf-litter decomposition and N mineralization in litterbags, placed across Canada: A 5-model comparison. *Ecol. Model.* 3:342–360.

Zhang, C.F., F.R. Meng, J.A. Trofymow, et al. 2007. Modeling mass and nitrogen remaining in litterbags for Canadian forest and climate conditions. *Can. J. Soil Sci.* 87:413–432.